HHS Public Access

Author manuscript

DNA Repair (Amst). Author manuscript; available in PMC 2018 December 01.

Published in final edited form as:

DNA Repair (Amst). 2017 December ; 60: 52–63. doi:10.1016/j.dnarep.2017.10.007.

XRCC1-mediated repair of strand breaks independent of PNKP binding

Julie K. Horton[1], **Donna F. Stefanick**[1], **Ming-Lang Zhao**[1], **Agnes K. Janoshazi**[2], **Natalie R. Gassman**[1,3], **Hannah J. Seddon**[1], and **Samuel H. Wilson**[1,*]

[1]Genomic Integrity and Structural Biology Laboratory, NIEHS, National Institutes of Health, Research Triangle Park, North Carolina 27709, USA

[2]Signal Transduction Laboratory, NIEHS, National Institutes of Health, Research Triangle Park, North Carolina 27709, USA

Abstract

Repair of DNA-protein crosslinks and oxidatively damaged DNA base lesions generates intermediates with nicks or gaps with abnormal and blocked 3′-phosphate and 5′-OH ends that prevent the activity of DNA polymerases and ligases. End cleaning in mammalian cells by Tdp1 and PNKP produces the conventional 3′-OH and 5′-phosphate DNA ends suitable for completion of repair. This repair function of PNKP is facilitated by its binding to the scaffold protein XRCC1, and phosphorylation of XRCC1 by CK2 at several consensus sites enables PNKP binding and recruitment to DNA damage. To evaluate this documented repair process, a phosphorylation mutant of XRCC1, designed to eliminate PNKP binding, was stably expressed in *Xrcc1*$^{-/-}$ mouse fibroblast cells. Analysis of PNKP-GFP accumulation at micro-irradiation induced damage confirmed that the XRCC1 phosphorylation mutant failed to support efficient PNKP recruitment, whereas there was rapid recruitment in cells expressing wild-type XRCC1. Recruitment of additional fluorescently-tagged repair factors PARP-1-YFP, GFF-XRCC1, PNKP-GFP and Tdp1-GFP to micro-irradiation induced damage was assessed in wild-type XRCC1-expressing cells. PARP-1-YFP recruitment was best fit to two exponentials, whereas kinetics for the other proteins were fit to a single exponential. The similar half-times of recruitment suggest that XRCC1 may be recruited with other proteins possibly as a pre-formed complex. *Xrcc1*$^{-/-}$ cells are hypersensitive to the DNA-protein cross-link inducing agent camptothecin (CPT) and the DNA oxidative agent H_2O_2 due in part to compromised PNKP-mediated repair. However, cells expressing the PNKP interaction mutant of XRCC1 demonstrated marked reversal of CPT hypersensitivity. This reversal represents XRCC1-dependent repair in the absence of the phosphorylation-dependent PNKP

*Corresponding Author: Genomic Integrity and Structural Biology Laboratory, NIEHS, National Institutes of Health, 111 T.W. Alexander Drive, P.O. Box 12233, Research Triangle Park, NC 27709, USA. Tel.; +1 919 541 4701; fax: +1 919 541 4724. wilson5@niehs.nih.gov (S.H. Wilson).

[3]Current address: Department of Oncologic Sciences, University of South Alabama Mitchell Cancer Institute, Mobile, Alabama 36604, USA

Conflict of Interest

The authors declare there is no conflict of interest.

recruitment and suggests either an XRCC1-independent mechanism of PNKP recruitment or a functional back-up pathway for cleaning of blocked DNA ends.

Keywords

XRCC1 phosphorylation; PNKP; PARP-1; Tdp1; Top1; camptothecin; hydrogen peroxide

1. Introduction

Utilizing a reversible covalent catalytic intermediate, topoisomerase 1 (Top1) nicks DNA and relaxes DNA supercoiling enabling transcription and replication. The covalent attachment of the catalytic tyrosine (Y723) of Top1 to the 3′-end of the nicked DNA terminus is referred to as a cleavable covalent complex (Top1cc). Under normal conditions, covalent binding is transient and religation of the incised DNA occurs. An inhibitor of Top1 activity, camptothecin (CPT), selectively prevents religation and stabilizes the covalent DNA-protein complex (DPC) [1]. The stalled Top1 complex can result in formation of replication-dependent double-strand breaks, which if not repaired by homologous recombination (HR) lead to cell death. Initial repair of the DPC requires targeted ubiquitination and proteolysis of Top1 to expose the phosphodiester bond between DNA and the residual Top1 Y723-linked peptide [2]. This is followed by tyrosyl DNA phosphodiesterase (Tdp1)-mediated hydrolysis of the Y723 DNA linkage leaving a blocking terminal 3′-phosphate. DNA end cleaning of the 3′-phosphate and phosphorylation of the 5′-OH by the bifunctional enzyme polynucleotide kinase 3′-phosphatase (PNKP) enables restoration of conventional DNA ends [3] and completion (i.e., ligation) of DPC repair (Fig. 1A).

Repair of endogenous and exogenous base lesions in cellular DNA occurs primarily by base excision repair (BER). Exposure of cells to the methylating agent, methyl methanesulfonate (MMS), results in methylation of DNA bases. These lesions are removed by a damage specific monofunctional glycosylase producing abasic (AP) sites that are cleaved by AP endonuclease 1 (APE1). The lyase activity of DNA polymerase β (pol β) is then critical for removing the 5′-deoxyribose (dRP) group, and the polymerase domain performs gap-filling DNA synthesis leaving a nicked substrate suitable for DNA ligation. The intracellular oxidant H_2O_2 can generate the highly reactive hydroxyl radical by the Fe^{2+}-dependent Fenton reaction [4]. H_2O_2 treatment of cells results in oxidatively generated DNA base damage following production of reactive oxygen species (ROS) in close proximity to DNA [5, 6]. Initiation of oxidative lesion repair by OGG1-mediated β-elimination results in AP sites, also 3′-dRP ends that are efficiently removed by APE1 resulting in 3′-OH and 5′-phosphate [7]. Alternatively, where BER of oxidatively damaged DNA is mediated by bifunctional NEIL DNA glycosylases with β,δ-elimination activity, PNKP functions to remove the blocking 3′-phosphate before pol β nucleotide insertion, and this 3′-phosphatase activity is essential for rapid repair [7–9]. Tdp1 can also hydrolyze 3′-phosphoglycolate produced during repair of H_2O_2-mediated oxidatively damaged DNA, and the resulting 3′-phosphate is further processed by PNKP [10].

XRCC1 is a multi-domain protein without catalytic activity, yet it interacts with a number of known repair proteins (Fig. 1B) facilitating and coordinating the repair of BER-induced indirect strand breaks and direct breaks requiring single strand break repair (SSBR) [11]. Interaction with phosphorylated XRCC1 enhances the activities of both Tdp1 and PNKP and facilitates repair of the Top1 DPC [12, 13]. Additionally, binding to XRCC1 is required to stabilize ligase IIIα (lig IIIα) *in vivo* [14, 15]. Thus, XRCC1 is involved in all stages of repair of CPT-induced DPC (Fig. 1A and B), and there is significant similarity with XRCC1-mediated SSBR [14, 16].

The ubiquitous protein kinase CK2, formerly known as casein kinase 2, is an essential constitutively active serine-threonine kinase able to phosphorylate hundreds of substrates associated with cellular stress responses [17, 18]. CK2 phosphorylation of XRCC1 at several consensus sites in the linker region between the BRCT I and BRCT II domains of the protein (Fig. 1B) [19, 20] is reported to be initiated by DNA damage [21]. Phosphorylated XRCC1 interacts with the forkhead-associated (FHA) domain of PNKP stimulating its activity and coordinating PNKP recruitment for BER and SSBR [19, 22]. Mutation of the eight primary CK2 consensus sites in XRCC1 prevents the interaction of XRCC1 with PNKP [23], and phosphorylation of XRCC1 stimulates PNKP recruitment to damage sites, and *in vitro* SSBR reactions [19, 23]. Thus, the phosphorylation status of XRCC1 influences PNKP-mediated repair, where inefficient repair may lead to formation of double-strand breaks and cell death.

Detection of DNA nicks (e.g., after CPT treatment) by PARP-1, as well as SSBs and other repair intermediates results in PARP-1 activation with synthesis of PAR polymers onto itself and other repair proteins [24]. PARP-1 affects Top1 nuclear dynamics, and PARylation of Top1 has a role in recruitment of Tdp1 [25]. Further, the N-terminal domain of Tdp1 binds the C-terminal domain of PARP-1 and PARylation of Tdp1 enhances its recruitment to DNA damage [26]. Cells not expressing PARP-1 have lesser Tdp1 activity [2]. The PARP-1-Tdp1 complex is also involved in XRCC1 recruitment to DNA damage [25]. Additionally, the ADP-ribose of PAR-modified PARP mediates recruitment of XRCC1 to SSBs and repair intermediates of damaged DNA bases via its BRCT I auto-modification domain [20, 27, 28], suggesting partially overlapping roles for PARP and Tdp1 in XRCC1 recruitment. The FHA domain of PNKP is also reported to interact with PAR [29], and this signals for recruitment of PNKP. Thus, PARP-1 is also involved in all stages of repair of CPT-induced DPC. Hypersensitivity to CPT has been observed in XRCC1-deficient CHO cells [13, 14] and *Xrcc1*$^{-/-}$ MEFs CPT [30], in *PARP-1*$^{-/-}$ MEFs [2] and in *Tdp1*$^{-/-}$ DT40 cells and Tdp1 knock down human cells [31, 32].

Here, we first confirmed recruitment in wild-type XRCC1-expressing (XC5) cells of fluorescently tagged proteins involved in repair of CPT-induced DPC. Since the role of PNKP and the importance of the PNKP interaction with phosphorylated XRCC1 is well documented, we made use of a CK2 phosphorylation mutant of XRCC1 designed to eliminate binding of PNKP [23] to evaluate repair independent of the XRCC1-PNKP interaction. This XRCC1 phosphorylation mutant was stably expressed in *Xrcc1*$^{-/-}$ cells, and the cells were characterized and compared with XC5 cells regarding repair protein expression and recruitment following damage by micro-irradiation. Cellular hypersensitivity

to CPT, the DNA oxidative agent H_2O_2, the DNA methylating agent MMS and other DNA damaging agents was also investigated. Additionally, the effect of a PARP inhibitor (PARPi) on CPT cellular sensitivity was examined.

2. Materials and methods

2.1. Cell culture and isolation of phosphorylation-mutant and wild-type complemented XRCC1 cells

Xrcc1$^{+/+}$ and *Xrcc1*$^{-/-}$ p53-deficient mouse embryonic fibroblasts (MEFs) were obtained from Dr. Robert Tebbs [33]. These cells were maintained in low glucose DMEM (Invitrogen) supplemented with 10% FBS at 37 °C. A large proportion of cellular XRCC1 is phosphorylated, and mutation of multiple CK2 phosphorylation sites of XRCC1 prevents interaction with PNKP [23]. A pEF-DEST51 vector-containing mouse XRCC1 cDNA (pXR1) was created as described previously [34]. Mutations at S517A, T518A, T522A, and S524A (equivalent to human S518A, T519A, T523A and S525A) were introduced by site-directed mutagenesis of the pXR1 wild-type vector to produce pXPK. Additional mutations at mouse S474A, S484A, and T487A (equivalent to S475A, S485A and T488A in human) were introduced by site-directed mutagenesis of the pXPK vector to produce pXCKD. The mammalian cell expression vectors were sequence verified.

One day before transfection, 2×10^5 *Xrcc1*$^{-/-}$ cells were seeded in six-well dishes in 2 ml of growth medium without antibiotics so that cells would be 95% confluent at the time of transfection. Complexes were prepared as follows: 5 μg of DNA was diluted in 250 μl of DMEM without serum and mixed gently. Lipofectamine™ 2000 (Invitrogen) was mixed gently prior to use then diluted by adding 10 μl to 250 μl of DMEM and incubated for 5 min at room temperature. The diluted DNA was combined with diluted Lipofectamine™ 2000, mixed gently and incubated for 20 min at room temperature. The complex mix was added to a dish of cells in serum-free medium (2 ml) and mixed gently, then incubated at 37°C in a 10% CO_2 incubator for 24 h. After transfection, cells were split into growth medium containing 10% FBS. Selection with blasticidin (10 μg/ml; Invitrogen) was initiated the following day and XCKD single cell clones were isolated and screened for XRCC1 expression by western blotting. Two independent clones (XCKD4 and 16) were used in this study.

Complementing mouse wild-type XRCC1 was expressed in *Xrcc1*$^{-/-}$ cells using lentivirus as described previously [35]. *Xrcc1*$^{-/-}$ cells were transduced with lentiviral particles at multiplicity of infection (MOI) of 20 per 50,000 cells, and stable cell lines were recovered after puromycin selection (6 μg/ml, Life Technologies). After characterization by western blot analysis (as described below), single cell XRCC1 WT clones were isolated from those demonstrating significant XRCC1 expression. Two clones (XC5 and XC2) were chosen for further study. Lentiviral knock down of pol β in XCKD16 was conducted as described for XRCC1 cells [30]. As previously, two different shRNAs against pol β (shRNA-468 and shRNA-662 from Sigma-Aldrich) were used. XCKD16 cells were transduced with lentiviral particles at multiplicity of infection (MOI) of 5 or 25 per 50,000 cells, and stable cell lines recovered after puromycin selection were characterized by western blotting. Lentiviral plasmid pLKO.1 was used for nonspecific shRNA.

Tdp1$^{-/-}$ mouse fibroblast cells were generated by dissociation of 14-day embryos. A single clone of immortalized cells was infected with a lentivirus expressing FLAG-tagged TDP1 (*Tdp1*^{Comp}). Both cell lines were obtained from Dr. Larry Povirk [36], and grown in RPMI (Invitrogen) supplemented with 10% FBS at 37 °C. Mycoplasma testing was performed routinely on all cell lines using a MycoAlert® Mycoplasma detection kit (Lonza, Rockland, ME).

2.2. Western blot analysis

Whole cell extracts were prepared as described previously [37, 38]. Briefly, cell pellets were thawed then resuspened in buffer containing 10 mM Tris–HCl, pH 7.8, 200 mM KCl, 1 mM EDTA, 20% glycerol, 0.1% NP-40, 1 mM DTT, and protease inhibitors. The suspension was rotated for 1 h at 4 °C, and extracts were clarified by centrifugation in a microcentrifuge at full speed for 15 min at 4 °C. The protein concentration of extracts was determined by the Bio-Rad assay.

Extract samples (60 μg) were loaded onto 4–12% Bis-Tris NuPAGE gels (Invitrogen) and electrophoresed in NuPAGE MES running buffer at 4°C. Proteins were transferred to nitrocellulose filters in the cold for 4 h at 25 V and filters were blocked overnight at 4°C in 5% nonfat dry milk in Tris-buffered saline (TBS) with 0.1% Tween 20 (TBST). Transfer blots were first incubated for 2 h at room temperature or overnight at 4°C with mouse monoclonal anti-XRCC1 primary antibody (Thermo Fisher Scientific, 33-2-5). After washing, filters were incubated with goat anti-mouse IgG-horseradish peroxidase (HRP) conjugated secondary antibody (1:2,000–1:20,000 dilution, Bio-Rad) and visualized using Super Signal (Thermo Scientific). Blots were stripped in Restore Western Blot Stripping Buffer (Thermo Scientific), washed three times in TBST, and blocked in 5% nonfat dry milk/TBST overnight before probing similarly with other primary antibodies. These included 18S anti-pol β [39], anti-PNKP (Santa Cruz sc 166153), anti-ligase III-1F3 (GeneTex MS-LIG31-PX1), and mouse anti-human PARP-1 (BD Pharmingen 51–6639GR). Anti-phospho (518/519/523) XRCC1 (Bethyl Laboratories A300-059A) and anti-phospho (S485/T488) XRCC1 (Bethyl Laboratories A300–231A) were probed with goat anti-rabbit HRP conjugate. In other experiments examining knockdown of pol β in XCKD16 cells, blots were incubated for 2 h at room temperature with pol β 18S monoclonal antibody [39], then with secondary goat anti-mouse HRP. Mouse monoclonal anti α-tubulin, clone DM 1A (Sigma T-9026) was used as a loading control.

2.3. Immunofluorescence and micro-irradiation

For immunofluorescence (IF) studies, cells were seeded on 35 mm glass bottomed petri dishes containing an etched grid (MatTek, Ashland, MA) at 2×10^5 cells per dish and incubated for 24 h in growth medium supplemented with 10 μM BrdU. DNA single strand breaks (SSBs) and oxidized DNA base lesions, but not double strand breaks (DSBs), were specifically introduced by micro-irradiation with a fiber-coupled 355 nm Coherent laser (maximum power 60 mW) via objective 40x C-Apochromat NA 1.2 Korr FCS M27 at an intensity equivalent to 0.165 uJ calculated as previously [40]. The irradiation strip size, region of interest (ROI), was manually drawn 0.45 μm across the nucleus for 200 μs (100 scanning iterations).

Previous studies had established that peak XRCC1 and pol β recruitment occurs 1 min after micro-irradiation in MEFs [40, 41]. Cells were fixed in 4% paraformaldehyde 1 min after irradiation and stained for IF. After fixation, cells were permeabilized with 0.25% Triton X-100 in PBS for 10 min, washed three times with PBS, then further permeabilized in 1% SDS for 5 min at 37 °C, washed six times with PBS, then blocked with 3% BSA in PBS for 60 min. Cells were then incubated with anti-XRCC1 antibody (1:50; Abcam ab1838), anti-PADPR antibody (1:100; Abcam ab14460) and anti-pol β antibody (1:200, Abcam ab26343) for 1 h. Cells were washed three times with PBS, then incubated with Alexa 488 conjugated anti-mouse, Alexa 647 conjugated anti-chicken and Alexa 546 conjugated anti-rabbit secondary antibodies (1:2,000; Life Technologies) for 1 h and cells were again washed three times with PBS. Fluorescence images were acquired with 512 × 512 pixels, bidirectional mode averaging of 2 lines, zoom 1.0 and pixel dwell time 3.5 μs with the same 40× water immersion objective on the Zeiss LSM780 microscope controlled by Zen 2012 SP2 software. Recruitment of XRCC1 and pol β, and synthesis of PAR at the site of DNA damage was analyzed using IMAGEJ and SigmaPlot (Systat Software Inc.) as described previously [40]. Each experiment was repeated, and images presented are representative.

Recruitment of C-terminal TurboGFP-tagged proteins (Origene) was assessed in XC5 cells following transient transfection. These were mouse XRCC1-GFP (MG209603), human PNKP-GFP (RG207551) and human Tdp1-GFP (RG214927). Recruitment of C-terminal PARP-1-YFP (obtained from PECF core, NIEHS) was also analyzed. XC5 cells were transiently transfected 24 h after plating using Lipofectamine^{TM} 2000 in medium supplemented with 10 μM BrdU (Sigma-Aldrich). 24 h after transfection, medium was changed to fresh room temperature growth medium without BrdU. Only cells with similar low to moderate fluorescence intensities were analyzed. DNA SSBs and DNA base lesions were introduced by micro-irradiation with a fiber–coupled 355 nm Coherent laser at maximum power (60 mW, 100% output) using a one pixel width strip (0.45 μM) per nucleus and an irradiation time of 200 μs (100 scanning iterations) as described above.

For image acquisition in live-cell experiments with GFP-tagged reporters, a 488 nm laser was used at 1% intensity to minimalize photo bleaching. For GFP, fluorescence emission was detected in the range of 491–580 nm using a pinhole of 40 μm. For YFP, a 514 nm laser was used and fluorescence emission detected with a bandpass filter from 520–610 nm for image acquisition. Fluorescence of protein recruitment was recorded by a highly sensitive, new generation Gallium arsenide phosphide (GaAsP) detector in photon counting mode, giving an order of magnitude more sensitivity than other photomultipliers in integral mode. This set up was necessary since fluorescent protein recruitment was not observed in cells with very high intensity expression. Samples were imaged using the same 40× C-Apochromat NA 1.2 Korr FCS M27 water immersion objective coupled to a Zeiss LSM780 confocal microscope (Carl Zeiss MicroImaging).

Three pre-bleach images were acquired to establish a base line prior to damage induction. Images were then acquired at room temperature every 1–3 s after the bleaching event for 200 s. Relative recruitment of fluorescent reporter was determined by measuring the signal intensity of GFP (or YFP) at the induced damage site using the ROI. Each experiment was repeated on at least 15 cells and analyzed using SigmaPlot. Time-lapse recruitment curves

were corrected by subtracting the post bleach signal intensity of the entire nucleus excluding the ROI. After intensity normalization setting the amplitudes of curves in the range 0–100%, data were plotted as mean normalized intensity ± SEM and fitted to a single or double exponential.

PARP-1 can be recruited and activated to produce PAR by both SSBs (including nicks) and DSBs [42]. To verify the absence of formation of DSBs in cells irradiated as described above (100 iterations) and able to recruit transiently transfected XRCC1-GFP to damage sites, they were stained for production of γH2AX with anti-phospho-H2AX monoclonal antibody. Other cells were irradiated with 1000 iterations as positive controls for DSBs and γH2AX staining. The position of cells on the etched grid of the dish was noted prior to irradiation and XRCC1-GFP recruitment. Cells were fixed in 4% paraformaldehyde at times 100 – 600 s after irradiation. Fixed cells were permeabilized with 0.25% Triton X-100 and then 1% SDS as described above. After washing with PBS, and blocking with 3% BSA, cells were incubated with anti-phospho-H2AX antibody, clone JBW301 (1:500; EMD Millipore 05–636) for 1 h at room temperature. Cells were again washed with PBS, then incubated with Alexa 647 conjugated anti-mouse secondary antibody (1:2,000; Life Technologies) for 1 h and again washed with PBS. Fluorescence images (GFP and Alexa 647) of damaged cells were acquired as before. Representative images are shown (Fig. S1).

In other experiments PNKP-GFP recruitment was compared in XC5, *Xrcc1*$^{-/-}$ and XCKD16 cell lines. Data were presented as raw fluorescence intensity ± SEM over the 200 s time course. Each experiment was repeated using at least sixteen cells. PNKP-GFP recruitment was also compared in Tdp1-KO and Tdp1-COMP cells. Data from at least eighteen cells were presented as normalized fluorescence intensity I_{max}/I_0, mean ± SEM, where I_{max} is the maximal fluorescence intensity indicating the maximal concentration of GFP-tagged protein recruited to the irradiated site, and I_o is the fluorescence intensity at the first time point of protein recruitment after UV irradiation. Normalization is a basic statistical operation used to scale heterogeneous sets of data, so that they can be readily compared. The effect of treatment with the PARPi veliparib on recruitment of XRCC1-GFP and PNKP-GFP was also assessed. Transfected XC5 cells were either pre-treated or not for 1 h with veliparib (10 μM), then irradiated in stripes. Recruitment of XRCC1-GFP and PNKP-GFP was followed for 200 s still in the absence or presence of inhibitor. Data are presented as normalized fluorescence intensity I_{max}/I_0, mean ± SEM.

2.4. Cytotoxicity studies by growth inhibition assay

Cells were seeded (10,000 – 30,000 cells per well in six-well dishes) in medium without selection antibiotic. The next day, cells were treated for 1 h with a range of concentrations of MMS (Sigma) or H_2O_2 (Fisher Scientific), or for 24 h with the Top1 inhibitor CPT (Sigma) or the thymidine analog 5-hydroxymethyl-2′-deoxyuridine (hmdUrd; Sigma). In other studies, cells were dosed with a combination of CPT plus the PARPi, 4-amino-1,8-naphthalimide (4-AN; Fisher Scientific; 5 μM for 24 h). After washing as appropriate, growth medium was added. Triplicate wells for each drug concentration were counted by a cell lysis procedure [38, 43] when untreated cells were 80% confluent, and results expressed as % control growth. Fold hypersensitivity was determined at IC_{90} concentrations, the dose

required for 90% decrease in cell growth. For experiments with mouse fibroblasts, we find this growth inhibition assay to be more reliable and consistent than clongenic or short-term cytotoxicity assays. Results obtained are in agreement with alternate assay methods [38].

3. Results

3.1. Recruitment of YFP and GFP-tagged repair proteins after laser irradiation

Repair of CPT-induced covalent DPC involves Tdp1, PARP-1, XRCC1, and PNKP among other factors such as lig IIIα (Fig 1A) [25, 26]. Recruitment of these four key repair factors in wild-type XRCC1 complemented XC5 cells was measured following laser micro-irradiation. Typical images representing accumulation at damaged sites after 100 s are shown in Fig. 2A for PARP-1-YFP, XRCC1-GFP, PNKP-GFP and Tdp1-GFP. Negative control experiments made use of enhanced GFP (eGFP) and no recruitment was detected (Fig. 2A). Note that fluorescence intensity increases only in the ROI surrounding the induced damaged site. Only cells with similar low to moderate intensities were used; no fluorescent protein recruitment was observed in cells with high intensity expression. With our protocol and laser settings (100 iterations), DNA SSBs and oxidatively generated base lesions, but not DSBs, are produced (Fig. S1). There was no detectable signal in cells stained with anti-γH2AX antibody under conditions where XRCC1-GFP can be recruited at times 100–600 s after damage. In contrast, staining with anti-γH2AX antibody was readily observed following higher intensity laser damage (1000 iterations) (Fig. S1). Recruitment of fluorescently tagged XRCC1 was expected (Fig. 2C) since recruitment of this protein had been identified by IF under the same conditions [35]. Importantly, PARP-1-YFP, PNKP-GFP and Tdp1-GFP were also recruited (Fig. 2B, D and E).

Analysis of recruitment data obtained from the time-course of PARP-1-YFP accumulation was best fit to two exponentials (Fig. 2B). The initial fast half-time was 4.3 ± 1 s for 13% of the amplitude and the second slower half-time was 26.8 ± 0.6 s for 77% of the amplitude. It was unexpected to observe recruitment consistent with two separate and distinct components for PARP-1 (Table 1) since PARP-1 is regarded as a first responder to DNA damage [42]. Recruitment of the second more abundant PARP-1 component was slower than that of the other proteins studied (Table 1). Recruitment kinetics for the other three proteins were fit to a single exponential. The half-time for XRCC1-GFP recruitment was 11.1 ± 0.1 s (Fig. 2C), for PNKP-GFP 13.6 ± 0.2 s (Fig. 2D) and for Tdp1 11.6 ± 0.7 s (Fig. 2E). Tdp1-GFP was recruited to a lower level than the other proteins studied in part because Tdp1 was not well retained at the damaged site (Fig. 2E). In these studies, Tdp1 is not recruited for a role in hydrolysis following Top1 proteolysis in DPC repair. However, Tdp1 can readily hydrolyze SSB ends and intermediates of repair of oxidatively generated base lesions induced by laser micro-irradiation [44]. A direct comparison with eGFP confirmed that Tdp1 recruitment is well above background (eGFP) levels (Fig. S2).

The plots of % normalized fluorescence over time in Figure 2 represent data from at least fifteen cells. A summary and comparison of recruitment half-times is presented in Table 1. The half-time for pol β-GFP recruitment was published previously [35] but was now reanalyzed in thirty XC5 cells under identical image acquisition conditions (Table 1 and Fig. S3). The recalculated recruitment half-time for pol β-GFP (11.1 ± 0.2 s) is similar to that of

XRCC1 and Tdp1, and these results are consistent with the possibility that these proteins may be recruited together, even as a pre-formed complex.

In control experiments using XRCC1-GFP transfection, recruitment half-time was found independent of cellular expression level in low to moderate intensity cells (Fig. S4), whereas fluorescence amplitude showed dependence. Two data sets of XRCC1-GFP experiments were compared; higher amplitude (12.9 ± 0.2) and lower amplitude (4.9 ± 0.4) (Fig. S4A), with average nuclear expression level as measured by fluorescence intensity of 48.6 ± 2.8 and 39.9 ± 2.8, respectively. The recruitment half-times of each group were similar, 11.1 ± 0.4 s and 11.8 ± 0.4 s, respectively. When all data were combined (n = 30), the half-time of XRCC1-GFP recruitment was 11.1 ± 0.1 s (Fig. S4B, Table 1).

To determine whether Tdp1 was involved in accumulation of PNKP to damage sites, recruitment of PNKP-GFP was compared in *Tdp1*$^{-/-}$ and *Tdp1*^{comp} cells (n = 18–20). These cells are described and were a kind gift from Dr. Larry Povirk [36]. The results suggest there was lesser recruitment of PNKP in the absence of Tdp1, but the recruitment kinetics were similar. Additionally, the accumulated PNKP remained stable for a longer time in Tdp1-expressing cells (Fig. S5), indicating that Tdp1 influenced PNKP recruitment, but was not required.

3.2. Characterization of XRCC1 phosphorylation mutant-expressing cells

A large proportion of cellular XRCC1 is phosphorylated, and mutation of multiple CK2 phosphorylation sites of XRCC1 prevents interaction with PNKP [23]. CK2-mediated phosphorylation of human XRCC1 at S518, T519, and T523 has only a minor role in modulation of PNKP binding to XRCC1 [45]. However, phosphorylation of additional sites in the linker region between the BRCT I and BRCT II domains of human XRCC1 (S475, S485 and T488) greatly stimulates the XRCC1-PNKP interaction [23]. Mutations of mouse S517A, T518A, T522A, and S524A (equivalent to human S518A, T519A, T523A and S525A) and mouse S474A, S484A, and T487A (equivalent to S475A, S485A and T488A in human) were introduced in XRCC1 by site-directed mutagenesis and this seven-site phosphorylation mutant was stably expressed in *Xrcc1*$^{-/-}$ cells. One of the selected clones (XCKD16) was chosen for further study based on expression level of XRCC1.

A clone of wild-type XRCC1-expressing cells (XC5) chosen for comparison studies expressed a similar level of XRCC1 as the selected phosphorylation mutant clone (XCKD16) (Fig. 3A, compare lanes 3 and 5). Both stably transfected clones had approximately 2-fold higher levels of expression than the parental *Xrcc1*$^{+/+}$ cells. Western blotting with phospho-specific XRCC1 antibodies (human S518/T519/T523 and S485/T488) revealed phosphorylation at both sites in *Xrcc1*$^{+/+}$ and XC5 cells, but at neither site in XCKD16 cells (Fig. 3A, lane 5). XCKD16 cells had a similar level of pol β as *Xrcc1*$^{+/+}$ (Fig. 3A, compare lanes 4 and 5). *Xrcc1*$^{-/-}$ cells were deficient in lig IIIα (Fig. 3A, lane 2), anticipated because XRCC1 is required for stabilization of this ligase through interaction at the BRCT II domain [46]. Surprisingly, since the BRCT II domain was not changed in the phosphorylation mutant, expression did not allow full expression of lig IIIα (Fig. 3A, lane 5). In general, lig IIIα is not believed to function in XRCC1-mediated nuclear DNA repair [47, 48]. However, lig IIIα can also act as a strand break sensor involved in recruitment of

XRCC1 and PNKP to sites of DNA damage caused by a Top1 inhibitor [49]. By this latter mechanism, lig IIIα deficiency (in *Xrcc1*$^{-/-}$ and XCKD16) would hinder recruitment of repair proteins and sensitize cells. Increased CPT sensitivity is observed in *Xrcc1*$^{-/-}$ cells, but hypersensitivity wa significantly reversed in XCKD16 suggesting that lig IIIα deficiency is not responsible for the observed CPT hypersensitivity. It is not clear why the level of PARP-1 was higher in *Xrcc1*$^{+/+}$ cells (Fig. 3A). The other variants with lower PARP-1 levels were isolated following transfection of *Xrcc1*$^{-/-}$ cells (Fig. 3A). *Xrcc1*$^{+/+}$, *Xrcc1*$^{-/-}$, XCDK16 and XC5 MEFs all expressed similar levels of PNKP (Fig. 3B).

Recruitment of XRCC1 and pol β, and synthesis of PAR at the site of UV micro-irradiation DNA damage was analyzed by IF in XC5, XCDK16 and *Xrcc1*$^{-/-}$ cells (Fig. 4). Synthesis of PAR 1 min after DNA damage was apparent in the three cell lines. Under these irradiation conditions and at this time point, there was no evidence for formation of DSBs (Fig. S1). In both XC5 and XCKD16 cells, the IF signal obtained for XRCC1 demonstrated that the XRCC1 phosphorylation mutant was recruited to PAR in a similar fashion to wild-type XRCC1. This XRCC1 result is in contrast to a previous report where recruitment of XRCC1 to sites of DNA damage was dependent on CK2 phosphorylation [50]. As expected, no XRCC1 signal was observed in *Xrcc1*$^{-/-}$ cells, but additionally pol β recruitment was not detected in these XRCC1-deficient cells (Fig. 4). There is evidence that an interaction between XRCC1 and pol β is required for recruitment of pol β to sites of DNA damage [19, 34]. Recruitment of pol β in XCDK16 cells indicates that this phosphorylation mutant is able to bind pol β.

3.3. Recruitment of PNKP-GFP in XRCC1 mutant cells after laser irradiation

XC5, XCKD16 and *Xrcc1*$^{-/-}$ cell lines were transiently transfected with PNKP-GFP and incubated with the sensitizer BrdU as above, and then laser irradiated the following day. A comparison of PNKP-GFP recruitment in XC5, XCDK16 and *Xrcc1*$^{-/-}$ cells at 0 and 240 s is presented in Fig. 5A where representative cells are shown. The combined data from 16–17 cells of each type are represented graphically (Fig. 5B). Under these micro-irradiation conditions and times up to 600 s, there was no evidence for formation of DSBs (Fig. S1). As noted in Figure 2D, there was rapid recruitment of PNKP-GFP to sites of damage in XC5 cells. Over the same time course, there was minimal recruitment in cells expressing the XRCC1 phosphorylation mutant (XCKD16) or in *Xrcc1*$^{-/-}$ MEFs where XRCC1 is absent (Fig. 5B). The experiment was repeated with an alternate set of clones (XC2 and XCKD4) and similar results (n = 15) were obtained and are presented in Figure S7A. The data confirm that interaction with phosphorylated XRCC1 is a requirement for PNKP recruitment to laser-induced DNA damage. In a previous publication describing a point mutation in human XRCC1 (A482T) that prevents PNKP binding, there was no change in initial recruitment of mutant compared with wild-type YFP-PNKP in HeLa cells, but retention at damaged sites was reduced [51]. The differences compared with results reported here may be due to the absence of phosphorylation in the additional XRCC1 phosphorylation mutant sites and use of C-terminal PNKP-GFP [51]. The retention after initial recruitment of these damage repair factors was not further addressed in this study.

3.4. Cell survival following exposure to DNA damaging agents

XRCC1-deficient cell lines are hypersensitive to CPT [13, 14]. MEFs were treated with a range of concentrations of CPT for 24 h and cell survival was measured by a growth inhibition assay (Fig. 1B). *Xrcc1*$^{-/-}$ cells demonstrated a 5.6-fold hypersensitivity (at IC_{90} concentrations) to CPT compared with *Xrcc1*$^{+/+}$ cells (Fig. 1B and 6A). Expression of wild-type XRCC1 (XC5 cells) fully rescued the hypersensitivity of *Xrcc1*$^{-/-}$ cells to CPT (Fig. 6A). Repair of the CPT-trapped Top1 DPC involves end cleaning by PNKP [13] and XRCC1 phosphorylation is required for recruitment of PNKP (Fig. 5B). Yet, the XCKD16 phosphorylation mutant-expressing cells demonstrated marked reversal of CPT hypersensitivity (shift from 5.7 to 3.6-fold sensitivity) (Fig. 6A and Table 2). Experiments were repeated with an alternate phosphorylation mutant clone (XCKD4), both cell lines had nearly identical sensitivity to CPT (Fig. S7B). The reversal of CPT hypersensitivity in XCKD16 and XCKD4 cells represents XRCC1-dependent repair in the presence of only negligable PNKP recruitment (Fig. 5B). The results suggest cellular recruitment of PNKP independent of interaction with XRCC1 or a functional back-up pathway for cleaning of blocked DNA ends.

BER of H_2O_2-induced oxidative DNA damage mediated by bifunctional NEIL DNA glycosylases requires PNKP to remove the 3′-phosphate repair intermediate before pol β nucleotide insertion [7]. *Xrcc1*$^{-/-}$ MEFs demonstrate hypersensitivity to H_2O_2 (Fig. 6B), and XCDK16 cells showed only limited reversal of this hypersensitivity. The result confirms that the phosphorylated XRCC1-PNKP interaction plays a significant role in repair and protection against H_2O_2-induced oxidative damage. In contrast, expression of the XRCC1 phosphorylation mutant allowed complete complementation of MMS and hmdUrd hypersensitivity (Fig. S6A and B). Expression of wild-type XRCC1 (XC2 cells) similarly complemented MMS hypersensitivity (Fig. S7C). In contrast to the wide array of DNA adducts formed following MMS exposure, hmdUrd is incorporated into DNA and elicits cytotoxicity only when removed by the glycosylase SMUG1 to initiate pol β-and XRCC1-dependent BER [52]. Studies of PNKP down-regulation in human lung carcinoma cells resulted in low level sensitization to CPT and H_20_2, but unexpectedly also to MMS [53]. Here, AP sites generated as intermediates of MMS repair may be channeled into a NEIL-PNKP pathway [54].

3.6. Effect of pol β knock down on cellular sensitivity to CPT

Previous experiments suggested that pol β-dependent BER is not important for repair of CPT-induced DNA damage since pol β null cells demonstrated only minor hypersensitivity to CPT [55]. Yet single-nucleotide insertion has been observed in *in vitro* repair reactions utilizing PNKP substrates and human whole cell extracts [56]. To determine if pol β has a repair role under conditions of functional PNKP deficiency, pol β was knocked down by lentivirus in the XCKD16 cell line. A western blot detected pol β in the control pLKO.1 transduced cells (PLKO), but pol β constructs (β 468 and β 662) produced significant knock down at MOI of 5 and 25 (Fig. 7A). Sensitivity to CPT was assayed as before, comparing pLKO.1 and pol β shRNA-transduced cells. Both pol β knock down populations were more CPT resistant than PLKO cells, and also had very similar sensitivities (Fig. 7B). The results suggest that XCKD16 cells were protected from CPT cytotoxicity in the absence of pol β

and not further sensitized as anticipated. Interestingly, it had been shown that *Xrcc1*$^{+/+}$ cells became slightly more resistant to CPT following pol β knock down, whereas pol β knock down did not affect CPT sensitivity of *Xrcc1*$^{-/-}$ cells [30].

3.7. Sensitization to CPT by 4-AN

Previous studies had indicated that maximal sensitization by PARP inhibition occurs where there is formation of the 5′-dRP-containing intermediate of DNA repair (e.g., MMS-induced damage) that is removed by the 5′-dRP lyase activity of pol β (Table 3) [57]. Repair of a CPT-trapped Top1cc does not produce a 5′-dRP intermediate, but instead 3′-phosphate and 5′-OH requiring both 3′-phosphatase and 5′-kinase activities of PNKP (Fig. 1A). A low PARPi-mediated sensitization (approximately 2.5-fold), was observed in *XRCC1*$^{+/+}$ cells (Fig. 8A and Table 3). In contrast, there was no observable effect of the PARPi, 4-AN, on CPT sensitivity in *Xrcc1*$^{-/-}$ cells (Fig. 8A and Table 3). PAR-modified PARP mediates recruitment of XRCC1 [20, 29], and this was confirmed by the inability to recruit XRCC1-GFP to micro-irradiation damage in the presence of the clinically used PARPi veliparib (Fig. 9A). It has been proposed that Tdp1 and PARP-1 are in the same Top1cc repair pathway [26], and PARylation of Top1 and Tdp1 similarly enhance their recruitment to DNA damage [25, 26]. However, there is no evidence for this mechanism of sensitization in *Xrcc1*$^{-/-}$ MEFs (Fig. 8A). A slightly lesser (2.1-fold) 4-AN-mediated sensitization of XCKD16 to CPT was seen compared with wild-type cells (Fig. 8B and Table 3), suggesting that PAR-mediated recruitment of the mutant XRCC1 is involved in repair in the absence of PNKP binding. Over the 200 s time course monitored, veliparib inhibited recruitment of PNKP-GFP to micro-irradiation DNA damage in XC5 cells (Fig. 9B). Since PNKP recruitment is largely dependent on binding to XRCC1 (Fig. 5B), this effect may result from the observed inhibition of XRCC1 recruitment by PARPi (Fig. 9A). The FHA domain of PNKP directly interacts with PAR [29], and is an alternate mechanism for PNKP recruitment.

4. Discussion

Repair of DPC arising following treatment of cells with CPT involves proteolysis of Top1, Tdp1-mediated hydrolysis of the residual Top1-DNA bond and end cleaning by PNKP prior to ligation (Fig. 1A). PARP-1, as an early responder, recognizes and binds to strand breaks in DNA resulting in synthesis of PAR polymers onto itself and other repair proteins [24]. PARylated Top1 and has a role in recruitment of Tdp1 [25] and PARylation of Tdp1 enhances its recruitment to DNA damage [26]. The PARP-1-Tdp1 complex and PAR-modified PARP mediate recruitment of XRCC1. Through a functional interaction, XRCC1 enhances Tdp1 activity in cells [13], and phosphorylation of XRCC1 enables PNKP binding and activity [23]. The FHA domain of PNKP is also reported to interact with PAR [29]. These and other observations reflect a central role for both PARP-1 and XRCC1 in DPC repair.

Recruitment of four key fluorescently tagged repair factors (PARP-1-YFP, XRCC1-GFP, GFP-PNPK and Tdp1-GFP) was analyzed in XC5 cells following laser micro-irradiation. The similarity in recruitment half-time data for XRCC1, Tdp1 and pol β (Table 1) suggest that these repair proteins may be recruited together, possibly as a pre-formed complex.

While recruitment kinetics for three of the tagged proteins were fit to a single exponential, it was unexpected to observe two separate and distinct recruitment kinetics for PARP-1 (Table 1). Detection of strand breaks by PARP-1 and immediate synthesis of PAR is an initiating event of repair [28, 58], yet recruitment of the second more abundant component is slower than the other proteins studied (Table 1). Perhaps in the initial fast recruitment, PARP-1 rapidly binds DNA via its DNA binding domain, whereas later PARylated PARP-1 may bind to other components of repair. It has been proposed that in a second recruitment phase once PARP-1 is activated, PARP-1 can bind PAR via its BRCT domain [58]. Further characterization of the 'fast' and 'slow' forms of PARP-1 recruitment is underway.

Using IF analysis, signal obtained for XRCC1 in both XC5 and XCDK16 cells 1 min after laser irradiation (Fig. 4) demonstrates that the XRCC1 phosphorylation mutant can be recruited by PAR just as observed for wild-type XRCC1. This was anticipated since the phosphorylation mutations are in the linker region of XRCC1 (Fig. 1C) whereas recruitment of XRCC1 is via the automodified PARP-1 BRCT1 domain [20]. This result is in contrast to an earlier report of a requirement for conserved CK2 phosphorylation sites for XRCC1 localization at DNA damage [23]. Pol β was also recruited in both cell types. Whereas there is rapid recruitment of transiently transfected PNKP-GFP to damage sites in XC5 cells (Fig. 2D), there was minimal recruitment in XCKD16 and *Xrcc1*$^{-/-}$ cells (Fig. 5). The results confirm that PNKP is most efficiently recruited in the presence of phosphorylated XRCC1.

The MMS and ethyl methanesulfonate (EMS) hypersensitivity phenotypes of pol β- and XRCC1-deficient cell variants have been widely reported and are thought to be due to BER deficiency [33, 55, 59, 60], as measured by strand breaks [55] and accumulation of PAR [34, 40]. The interaction between XRCC1 and pol β is extremely important for recruitment of pol β to sites of BER intermediates [57]. Inefficient BER in *Xrcc1*$^{-/-}$ MEFs leads to extreme hypersensitivity to MMS (7.7 -fold) and hmdUrd (16 -fold) (Fig. S6A and B). Only minor CPT hypersensitivity is observed in pol β null cells and the hypersensitivity is not increased in *Xrcc1*$^{-/-}$ MEFs with a knock down of pol β [30], but single-nucleotide insertion has been reported *in vitro* when using PNKP substrates [56]. Pol β was knocked down in XCKD16 cells to identify any back-up role for pol β-dependent repair under conditions of PNKP functional deficiency. Unexpectedly, pol β knock down populations were not sensitized but became more CPT resistant (Fig. 7B). The result suggests that XCKD16 cells are in some way protected from CPT cytotoxicity in the absence of pol β. The effect is specific to XCKD16 cells since *Xrcc1*$^{+/+}$ cells became only minimally more resistant to CPT following pol β knock down [30].

Wild-type XRCC1 expressed in XC5 cells fully reverses CPT hypersensitivity of *Xrcc1*$^{-/-}$ cells (Fig. 6A), confirming that XRCC1 is essential for efficient repair of CPT-mediated Top1 DPC (Table 2). Repair of the CPT-trapped Top1 DPC requires end cleaning by PNKP [13] and PNKP activity is rate limiting in repair in XRCC1-deficient cells [61]. As noted above, there was negligible cellular recruitment of PNKP-GFP to micro-irradiation damage in XCKD16 cells (Fig. 5) in which XRCC1 is not phosphorylated (Fig. 3A), yet there was significant reversal of CPT hypersensitivity in XCDK16 cells (Fig. 6A and Table 2). Additional XRCC1 protein interactions remaining in the XCKD mutant facilitate accumulation and activity of Tdp1 [13], and stabilization of lig IIIα [14], that is also

involved in Top1-DPC repair. Cell lines from SCAN1 patients mutated in Tdp1 have decreased repair after incubation with either CPT or H_2O_2 [62]. However, disruption of interaction between XRCC1 and lig IIIα has been shown not to affect cell survival following treatment of cycling cells with simple alkylating agents [21, 63] and in general lig IIIα is not thought to be involved in nuclear DNA repair [47, 48].

Our results suggest a functional back-up or alternate repair pathway for cleaning of blocked DNA ends. APE1 has weak 3′-phosphatase activity, but is thought unlikely to contribute cellular activity [7]. Alternatively, recruitment of PNKP may be sufficient even in the absence of binding to XRCC1, although less efficient and not observed within 200 s in XRCC1 phosphorylation mutant cells (Fig. 5). It has been suggested that non-phosphorylated XRCC1 binding at the catalytic domain of PNKP as well as phosphorylated XRCC1 binding at the FHA domain can enhance the turnover rate of PNKP [22]. The FHA domain of PNKP also interacts with the iso-ADP-ribose linkage between each PAR ribose [29]. There is exploration of use of a PNKP small molecule inhibitor or targeting of the XRCC1-PNKP interaction in cancer therapy [64].

BER of oxidative damage following H_2O_2 exposure may be mediated by NEIL DNA glycosylases. In this situation, PNKP is required to remove the 3′-phosphate before pol β nucleotide insertion [7]. Whereas rates of repair of oxidative DNA damage were shown to be slowed in CHO cells expressing XRCC1 that cannot interact with PNKP, H_2O_2 hypersensitivity was fully rescued [9]. In contrast, XCDK16 cells showed only limited reversal of the H_2O_2 hypersensitivity of *Xrcc1*$^{-/-}$ MEFs (Fig. 6B). Expression of the XRCC1 phosphorylation mutant allowed complete complementation of MMS and hmdUrd hypersensitivity (Fig. S4A and B). This was anticipated since BER following damage by these agents requires XRCC1 but is unlikely to involve PNKP.

The PARPi 4-AN strongly sensitizes *Xrcc1*$^{+/+}$ cells, and to a lesser extent *Xrcc1*$^{-/-}$ cells, to MMS-induced cytotoxic 5′-dRP groups. [34] (Table 3). The considerably lesser PARPi-mediated sensitization to CPT compared with MMS in *XRCC1*$^{+/+}$ cells may result from lesser PARP activation and auto-PARylation with formation of 3′-OH and 5′-phosphate rather than a 5′-dRP intermediate of repair (Fig. 8A and Table 3). PARylated PARP is presumed essential for XRCC1 localization to DNA damage [29], and the clinically used PARPi veliparib prevented recruitment of XRCC1-GFP to micro-irradiation damage in XC5 cells (Fig. 9A). 4-AN-mediated sensitization of XCKD16 to CPT was observed at a level similar to that in *Xrcc1*$^{+/+}$ cells (Fig. 8B, Table 3), suggesting the involvement of PAR-mediated recruitment of the phosphorylation mutant of XRCC1 in repair. Veliparib strongly inhibited recruitment of PNKP-GFP to micro-irradiation DNA damage in XC5 cells (Fig. 9B). A lesser inhibition by another PARPi olaparib has been reported previously in wild-type MEFs [29]. It is possible that PARP inhibition prevents PNKP recruitment by the primary inhibition of XRCC1 recruitment (Fig. 9A).

Inhibition of PARylation of proteins other than PARP-1 that are involved in management of CPT-induced Top1cc could also result in enhanced cytotoxicity of CPT. PARylation of Top1 itself following CPT treatment mediates recruitment of Tdp1, XRCC1 and lig IIIα [25]. PAR polymers also regulate Top1 nuclear dynamics, and PARPi mediated increases in CPT

binding and formation of Top1cc could enhance CPT cytotoxicity [25]. The N-terminal domain of Tdp1 binds the C-terminal of PARP-1. PARylation of Tdp1 is reported to enhance its recruitment to trapped Top1cc and the formation of a Tdp1-PARP-1 complex is key for recruitment of XRCC1 [26]. Interestingly, PARP inhibition of *Tdp1*$^{-/-}$ cells, like *Xrcc1*$^{-/-}$ cells (Fig. 8A), did not sensitize them to CPT. Tdp1 and PARP-1 are epistatic for repair of Top1 cc [26], and presumably PARP and XRCC1 participate in the same repair pathway. Conversion of CPT-initiated Top1cc to cytotoxic DSBs can be prevented by reversal and restart of replication forks, a RECQ1 helicase-dependent procedure promoted by PARP activity [65]. Sensitization of cells by PARP inhibition could result from impairment of replication fork restart with formation of high levels of DSBs [65, 66] and supports the findings of synergistic effects of Top1 and PARP inhibitors [67].

Our results point to significant XRCC1-mediated repair of DPC under conditions of PNKP functional deficiency. Repair does not seem to involve pol β-dependent long patch BER, rather knock down of pol β enhanced cellular resistance (Fig 7). Knock down of PNKP in human cells resulted in accumulation of CPT-induced strand breaks [62] while mutations slowed repair [68]. Similarly, in a SCA3 mouse model with decreased PNKP activity, there was accumulation of unrepaired strand breaks, blockage of DNA replication and formation of replication-induced double strand breaks [69]. HR has a role as a back-up pathway in the absence of SSBR, but the requirement for removal of the 3′-blocking group still remains.

Acknowledgments

The authors thank Lois Wyrick and William Beard for help with figure preparation and Michael Howard for critically reading the manuscript. We are grateful to the NIEHS Viral Vector Core Facility for assistance with the lentivirus expression vectors, Robert Petrovich and the NIEHS Protein Expression Core Facility for assistance with expression vector construction, C. Jeff Tucker and Erica Scappini in the NIEHS Fluorescence Microscopy and Imaging Center for their expert assistance with micro-irradiation studies and the NIEHS Flow Cytometry Center for help with flow cytometric analysis.

Grant Support

This work was supported by the Intramural Research Program of the NIH, National Institute of Environmental Health Sciences (project numbers Z01 ES050158 and ES050159).

References

1. Pommier Y. Topoisomerase I inhibitors: camptothecins and beyond. Nat Rev Cancer. 2006; 6:789–802. [PubMed: 16990856]
2. Pommier Y, Barcelo JM, Rao VA, Sordet O, Jobson AG, Thibaut L, Miao ZH, Seiler JA, Zhang H, Marchand C, Agama K, Nitiss JL, Redon C. Repair of topoisomerase I-mediated DNA damage. Prog Nucleic Acid Res Mol Biol. 2006; 81:179–229. [PubMed: 16891172]
3. Weinfeld M, Mani RS, Abdou I, Aceytuno RD, Glover JN. Tidying up loose ends: the role of polynucleotide kinase/phosphatase in DNA strand break repair. Trends Biochem Sci. 2011; 36:262–271. [PubMed: 21353781]
4. El-Bahr SM. Biochemistry of free radicals and oxidative stress. Science Internat. 2013; 1:111–117.
5. Halliwell, B., Gutteridge, JMC. Methods Enzymol. Academic Press; 1990. Role of free radicals and catalytic metal ions in human disease: An overview; p. 1-85.
6. Jaruga P, Dizdaroglu M. Repair of products of oxidative DNA base damage in human cells. Nucleic Acids Res. 1996; 24:1389–1394. [PubMed: 8628669]

7. Wiederhold L, Leppard JB, Kedar P, Karimi-Busheri F, Rasouli-Nia A, Weinfeld M, Tomkinson AE, Izumi T, Prasad R, Wilson SH, Mitra S, Hazra TK. AP endonuclease-independent DNA base excision repair in human cells. Mol Cell Biol. 2004; 15:209–220.
8. Jilani A, Ramotar D, Slack C, Ong C, Yang XM, Scherer SW, Lasko DD. Molecular cloning of the human gene, PNKP, encoding a polynucleotide kinase 3′-phosphatase and evidence for its role in repair of DNA strand breaks caused by oxidative damage. J Biol Chem. 1999; 274:24176–24186. [PubMed: 10446192]
9. Breslin C, Caldecott KW. DNA 3′-phosphatase activity is critical for rapid global rates of single-strand break repair following oxidative stress. Mol Cell Biol. 2009; 29:4653–4662. [PubMed: 19546231]
10. Inamdar KV, Pouliot JJ, Zhou T, Lees-Miller SP, Rasouli-Nia A, Povirk LF. Conversion of phosphoglycolate to phosphate termini on 3′ overhangs of DNA double strand breaks by the human tyrosyl-DNA phosphodiesterase hTdp1. J Biol Chem. 2002; 277:27162–27168. [PubMed: 12023295]
11. Caldecott KW. XRCC1 and DNA strand break repair. DNA Repair. 2003:955–969. [PubMed: 12967653]
12. Whitehouse CJ, Taylor RM, Thistlethwaite A, Zhang H, Karimi-Busheri F, Lasko DD, Weinfeld M, Caldecott KW. XRCC1 stimulates human polynucleotide kinase activity at damaged DNA termini and accelerates DNA single-strand break repair. Cell. 2001; 104:107–117. [PubMed: 11163244]
13. Plo I, Liao ZY, Barcelo JM, Kohlhagen G, Caldecott KW, Weinfeld M, Pommier Y. Association of XRCC1 and tyrosyl DNA phosphodiesterase (Tdp1) for the repair of topoisomerase I-mediated DNA lesions. DNA Repair. 2003; 2:1087–1100. [PubMed: 13679147]
14. Barrows LR, Holden JA, Anderson M, D'Arpa P. The CHO XRCC1 mutant, EM9, deficient in DNA ligase III activity, exhibits hypersensitivity to camptothecin independent of DNA replication. Mutat Res. 1998; 408:103–110. [PubMed: 9739812]
15. Caldecott KW, Tucker JD, Stanker LH, Thompson LH. Characterization of the XRCC1-DNA ligase III complex *in vitro* and its absence from mutant hamster cells. Nucleic Acids Res. 1995; 23:4836–4843. [PubMed: 8532526]
16. Brem R, Hall J. XRCC1 is required for DNA single-strand break repair in human cells. Nucleic Acids Res. 2005; 33:2512–2520. [PubMed: 15867196]
17. Sarno S, Ghisellini P, Pinna LA. Unique activation mechanism of protein kinase CK2. The N-terminal segment is essential for constitutive activity of the catalytic subunit but not of the holoenzyme. J Biol Chem. 2002; 277:22509–22514. [PubMed: 11956194]
18. Meggio F, Pinna LA. One-thousand-and-one substrates of protein kinase CK2? FASEB J. 2003; 17:349–368. [PubMed: 12631575]
19. Hanssen-Bauer A, Solvang-Garten K, Sundheim O, Pena-Diaz J, Andersen S, Slupphaug G, Krokan HE, Wilson DM 3rd, Akbari M, Otterlei M. XRCC1 coordinates disparate responses and multiprotein repair complexes depending on the nature and context of the DNA damage. Environ Mol Mutagen. 2011; 52:623–635. [PubMed: 21786338]
20. Kim IK, Stegeman RA, Brosey CA, Ellenberger T. A quantitative assay reveals ligand specificity of the DNA scaffold repair protein XRCC1 and efficient disassembly of complexes of XRCC1 and the poly(ADP-ribose) polymerase 1 by poly(ADP-ribose) glycohydrolase. J Biol Chem. 2015; 290:3775–3783. [PubMed: 25477519]
21. Kubota Y, Horiuchi S. Independent roles of XRCC1's two BRCT motifs in recovery from methylation damage. DNA Repair. 2003; 2:407–415. [PubMed: 12606121]
22. Lu M, Mani RS, Karimi-Busheri F, Fanta M, Wang H, Litchfeld DW, Weinfeld M. Independent mechanisms of stimulation of polynucleotide kinase/phosphatase by phosphorylated and non-phosphorylated XRCC1. Nucleic Acids Res. 2010; 38:510–521. [PubMed: 19910369]
23. Loizou JI, El-Khamisy SF, Zlatanou A, Moore DJ, Chan DW, Qin J, Sarno S, Meggio F, Pinna LA, Caldecott KW. The protein kinase CK2 facilitates repair of chromosomal DNA single-strand breaks. Cell. 2004; 117:17–28. [PubMed: 15066279]
24. Amé JC, Spenlehauer C, de Murcia G. The PARP superfamily. Bioessays. 2004; 26:882–893. [PubMed: 15273990]

25. Das SK, Rehman I, Ghosh A, Sengupta S, Majumdar P, Jana B, Das BB. Poly(ADP-ribose) polymers regulate DNA topoisomerase I (Top1) nuclear dynamics and camptothecin sensitivity in living cells. Nucleic Acids Res. 2016; 44:8363–8375. [PubMed: 27466387]
26. Das BB, Huang SY, Murai J, Rehman I, Amé JC, Sengupta S, Das SK, Majumdar P, Zhang H, Biard D, Majumder HK, Schreiber V, Pommier Y. PARP1-TDP1 coupling for the repair of topoisomerase I-induced DNA damage. Nucleic Acids Res. 2014; 42:4435–4449. [PubMed: 24493735]
27. El-Khamisy SF, Masutani M, Suzuki H, Caldecott KW. A requirement for PARP-1 for the assembly or stability of XRCC1 nuclear foci at sites of oxidative DNA damage. Nucleic Acids Res. 2003; 31:5526–5533. [PubMed: 14500814]
28. Campalans A, Kortulewski T, Amouroux R, Menoni H, Vermeulen W, Radicella JP. Distinct spatiotemporal patterns and PARP dependence of XRCC1 recruitment to single-strand break and base excision repair. Nucleic Acids Res. 2013; 41:3115–3129. [PubMed: 23355608]
29. Li M, Lu LY, Yang CY, Wang S, Yu X. The FHA and BRCT domains recognize ADP-ribosylation during DNA damage response. Genes Dev. 2013; 27:1752–1768. [PubMed: 23964092]
30. Horton JK, Gassman NR, Dunigan BD, Stefanick DF, Wilson SH. DNA polymerase β-dependent cell survival independent of XRCC1 expression. DNA Repair. 2015; 26:23–29. [PubMed: 25541391]
31. Murai J, Huang S-yN, Das BB, Dexheimer TS, Takeda S, Pommier Y. Tyrosyl-DNA Phosphodiesterase 1 (TDP1) repairs DNA damage induced by Topoisomerases I and II and base alkylation in vertebrate cells. J Biol Chem. 2012; 287:12848–12857. [PubMed: 22375014]
32. Alagoz M, Wells OS, El-Khamisy SF. TDP1 deficiency sensitizes human cells to base damage via distinct topoisomerase I and PARP mechanisms with potential applications for cancer therapy. Nucleic Acids Res. 2014; 42:3089–3103. [PubMed: 24335147]
33. Tebbs RS, Flannery ML, Meneses JJ, Hartmann A, Tucker JD, Thompson LH, Cleaver JE, Pedersen RA. Requirement for the Xrcc1 DNA base excision repair gene during early mouse development. Dev Biol. 1999; 208:513–529. [PubMed: 10191063]
34. Horton JK, Stefanick DF, Gassman NR, Williams JG, Gabel SA, Cuneo MJ, Prasad R, Kedar PS, DeRose EF, Hou EW, London RE, Wilson SH. Preventing oxidation of cellular XRCC1 affects PARP-mediated DNA damage responses. DNA Repair. 2013; 12:774–785. [PubMed: 23871146]
35. Horton JK, Seddon HJ, Zhao M-L, Gassman NR, Janoshazi AK, Stefanick DF, Wilson SH. Role of the oxidized form of XRCC1 in protection against extreme oxidative stress. Free Radic Biol Med. 2017
36. Hawkins AJ, Subler MA, Akopiants K, Wiley JL, Taylor SM, Rice AC, Windle JJ, Valerie K, Povirk LF. In vitro complementation of Tdp1 deficiency indicates a stabilized enzyme-DNA adduct from tyrosyl but not glycolate lesions as a consequence of the SCAN1 mutation. DNA Repair. 2009; 8:654–663. [PubMed: 19211312]
37. Biade S, Sobol RW, Wilson SH, Matsumoto Y. Impairment of proliferating cell nuclear antigen-dependent apurinic/apyrimidinic site repair on linear DNA. J Biol Chem. 1998; 273:898–902. [PubMed: 9422747]
38. Horton JK, Stefanick DF, Prasad R, Gassman NR, Kedar PS, Wilson SH. Base excision repair defects invoke hypersensitivity to PARP inhibition. Mol Cancer Res. 2014; 12:1128–1139. [PubMed: 24770870]
39. Singhal RK, Prasad R, Wilson SH. DNA polymerase β conducts the gap-filling step in uracil-initiated base excision repair in a bovine testes nuclear extract. J Biol Chem. 1995; 270:949–957. [PubMed: 7822335]
40. Gassman NR, Stefanick DF, Kedar PS, Horton JK, Wilson SH. Hyperactivation of PARP triggers nonhomologous end-joining in repair-deficient mouse fibroblasts. PLoS ONE. 2012; 7:e49301. [PubMed: 23145148]
41. Masaoka A, Gassman NR, Kedar PS, Prasad R, Hou EW, Horton JK, Bustin M, Wilson SH. HMGN1 protein regulates poly(ADP-ribose) polymerase-1 (PARP-1) self-PARylation in mouse fibroblasts. J Biol Chem. 2012; 287:27648–27658. [PubMed: 22736760]

42. Haince JF, McDonald D, Rodrigue A, Dery U, Masson JY, Hendzel MJ, Poirier GG. PARP1-dependent kinetics of recruitment of MRE11 and NBS1 proteins to multiple DNA damage sites. J Biol Chem. 2008; 283:1197–1208. [PubMed: 18025084]
43. Butler WB. Preparing nuclei from cells in monolayer cultures suitable for counting and for following synchronized cells through the cell cycle. Anal Biochem. 1984; 141:70–73. [PubMed: 6496937]
44. Pommier Y, Huang S-yN, Gao R, Das BB, Murai J, Marchand C. Tyrosyl-DNA-phosphodiesterases (TDP1 and TDP2). DNA Repair. 2014; 19:114–129. [PubMed: 24856239]
45. Luo H, Chan DW, Yang T, Rodriguez M, Chen BP, Leng M, Mu JJ, Chen D, Songyang Z, Wang Y, Qin J. A new XRCC1-containing complex and its role in cellular survival of methyl methanesulfonate treatment. Mol Cell Biol. 2004; 24:8356–8365. [PubMed: 15367657]
46. Taylor RM, Wickstead B, Cronin S, Caldecott KW. Role of a BRCT domain in the interaction of DNA ligase III-α with the DNA repair protein XRCC1. Curr Biol. 1998; 8:877–880. [PubMed: 9705932]
47. Gao Y, Katyal S, Lee Y, Zhao J, Rehg JE, Russell HR, McKinnon PJ. DNA ligase III is critical for mtDNA integrity but not Xrcc1-mediated nuclear DNA repair. Nature. 2011; 471:240–244. [PubMed: 21390131]
48. Simsek D, Furda A, Gao Y, Artus J, Brunet E, Hadjantonakis AK, Van Houten B, Shuman S, McKinnon PJ, Jasin M. Crucial role for DNA ligase III in mitochondria but not in Xrcc1-dependent repair. Nature. 2011; 471:245–248. [PubMed: 21390132]
49. Abdou I, Poirier GG, Hendzel MJ, Weinfeld M. DNA ligase III acts as a DNA strand break sensor in the cellular orchestration of DNA strand break repair. Nucleic Acids Res. 2015; 43:875–892. [PubMed: 25539916]
50. Kubota Y, Takanami T, Higashitani A, Horiuchi S. Localization of X-ray cross complementing gene 1 protein in the nuclear matrix is controlled by casein kinase II-dependent phosphorylation in response to oxidative damage. DNA Repair. 2009; 8:953–960. [PubMed: 19596613]
51. Della-Maria J, Hegde ML, McNeill DR, Matsumoto Y, Tsai MS, Ellenberger T, Wilson DM 3rd, Mitra S, Tomkinson AE. The interaction between polynucleotide kinase phosphatase and the DNA repair protein XRCC1 is critical for repair of DNA alkylation damage and stable association at DNA damage sites. J Biol Chem. 2012; 287:39233–39244. [PubMed: 22992732]
52. Boorstein RJ, Cummings A Jr, Marenstein DR, Chan MK, Ma Y, Neubert TA, Brown SM, Teebor GW. Definitive identification of mammalian 5-hydroxymethyluracil DNA *N*-glycosylase activity as SMUG1. J Biol Chem. 2001; 276:41991–41997. [PubMed: 11526119]
53. Rasouli-Nia A, Karimi-Busheri F, Weinfeld M. Stable down-regulation of human polynucleotide kinase enhances spontaneous mutation frequency and sensitizes cells to genotoxic agents. Proc Natl Acad Sci USA. 2004; 101:6905–6910. [PubMed: 15100409]
54. Hazra TK, Das A, Das SK, Choudhury S, Kow YW, Roy R. Oxidative DNA damage repair in mammalian cells: A new perspective. DNA Repair. 2007; 6:470–480. [PubMed: 17116430]
55. Horton JK, Watson M, Stefanick DF, Shaughnessy DT, Taylor JA, Wilson SH. XRCC1 and DNA polymerase β in cellular protection against cytotoxic DNA single-strand breaks. Cell Res. 2008; 18:48–63. [PubMed: 18166976]
56. Whiteside JR, Box CL, McMillan TJ, Allinson SL. Cadmium and copper inhibit both DNA repair activities of polynucleotide kinase. DNA Repair. 2010; 9:83–89. [PubMed: 19962355]
57. Horton JK, Wilson SH. Predicting enhanced cell killing through PARP inhibition. Mol Cancer Res. 2013; 11:13–18. [PubMed: 23193155]
58. Mortusewicz O, Amé JC, Schreiber V, Leonhardt H. Feedback-regulated poly(ADP-ribosyl)ation by PARP-1 is required for rapid response to DNA damage in living cells. Nucleic Acids Res. 2007; 35:7665–7675. [PubMed: 17982172]
59. Sobol RW, Horton JK, Kuhn R, Gu H, Singhal RK, Prasad R, Rajewsky K, Wilson SH. Requirement of mammalian DNA polymerase-β in base-excision repair. Nature. 1996; 379:183–186. [PubMed: 8538772]
60. Shen MR, Zdzienicka MZ, Mohrenweiser H, Thompson LH, Thelen MP. Mutations in hamster single-strand break repair gene XRCC1 causing defective DNA repair. Nucleic Acids Res. 1998; 26:1032–1037. [PubMed: 9461464]

61. Caldecott KW. Single-strand break repair and genetic disease. Nat Rev Genet. 2008; 9:619–631. [PubMed: 18626472]

62. El-Khamisy SF, Saifi GM, Weinfeld M, Johansson F, Helleday T, Lupski JR, Caldecott KW. Defective DNA single-strand break repair in spinocerebellar ataxia with axonal neuropathy-1. Nature. 2005; 434:108–113. [PubMed: 15744309]

63. Moore DJ, Taylor RM, Clements P, Caldecott KW. Mutation of a BRCT domain selectively disrupts DNA single-strand break repair in noncycling Chinese hamster ovary cells. Proc Natl Acad Sci USA. 2000; 97:13649–13654. [PubMed: 11095742]

64. Allinson SL. DNA end-processing enzyme polynucleotide kinase as a potential target in the treatment of cancer. Future Oncol. 2010; 6:1031–1042. [PubMed: 20528239]

65. Berti M, Ray Chaudhuri A, Thangavel S, Gomathinayagam S, Kenig S, Vujanovic M, Odreman F, Glatter T, Graziano S, Mendoza-Maldonado R, Marino F, Lucic B, Biasin V, Gstaiger M, Aebersold R, Sidorova JM, Monnat RJ Jr, Lopes M, Vindigni A. Human RECQ1 promotes restart of replication forks reversed by DNA topoisomerase I inhibition. Nat Struct Mol Biol. 2013; 20:347–354. [PubMed: 23396353]

66. Ray Chaudhuri A, Hashimoto Y, Herrador R, Neelsen KJ, Fachinetti D, Bermejo R, Cocito A, Costanzo V, Lopes M. Topoisomerase I poisoning results in PARP-mediated replication fork reversal. Nat Struct Mol Biol. 2012; 19:417–423. [PubMed: 22388737]

67. Murai J, Zhang Y, Morris J, Ji J, Takeda S, Doroshow JH, Pommier Y. Rationale for poly(ADP-ribose) polymerase (PARP) inhibitors in combination therapy with camptothecins or temozolomide based on PARP trapping versus catalytic inhibition. J Pharmacol Exp Ther. 2014; 349:408–416. [PubMed: 24650937]

68. Shen J, Gilmore EC, Marshall CA, Haddadin M, Reynolds JJ, Eyaid W, Bodell A, Barry B, Gleason D, Allen K, Ganesh VS, Chang BS, Grix A, Hill RS, Topcu M, Caldecott KW, Barkovich AJ, Walsh CA. Mutations in PNKP cause microcephaly, seizures and defects in DNA repair. Nat Genet. 2010; 42:245–249. [PubMed: 20118933]

69. Chatterjee A, Saha S, Chakraborty A, Silva-Fernandes A, Mandal SM, Neves-Carvalho A, Liu Y, Pandita RK, Hegde ML, Hegde PM, Boldogh I, Ashizawa T, Koeppen AH, Pandita TK, Maciel P, Sarkar PS, Hazra TK. The role of the mammalian DNA end-processing enzyme polynucleotide kinase 3′-phosphatase in spinocerebellar ataxia type 3 pathogenesis. PLoS Genet. 2015; 11:e1004749. [PubMed: 25633985]

Highlights

- End cleaning activities of PNKP facilitated by binding to phosphorylated XRCC1
- Expression of XRCC1 phosphorylation mutant designed to eliminate PNKP interaction
- Marked reversal of hypersensitivity to CPT-induced DNA-protein cross-links
- Possibility XRCC1 binding-independent recruitment of PNKP sufficient for repair
- Alternate PNKP-independent repair of the CPT-induced DNA-protein cross-links?

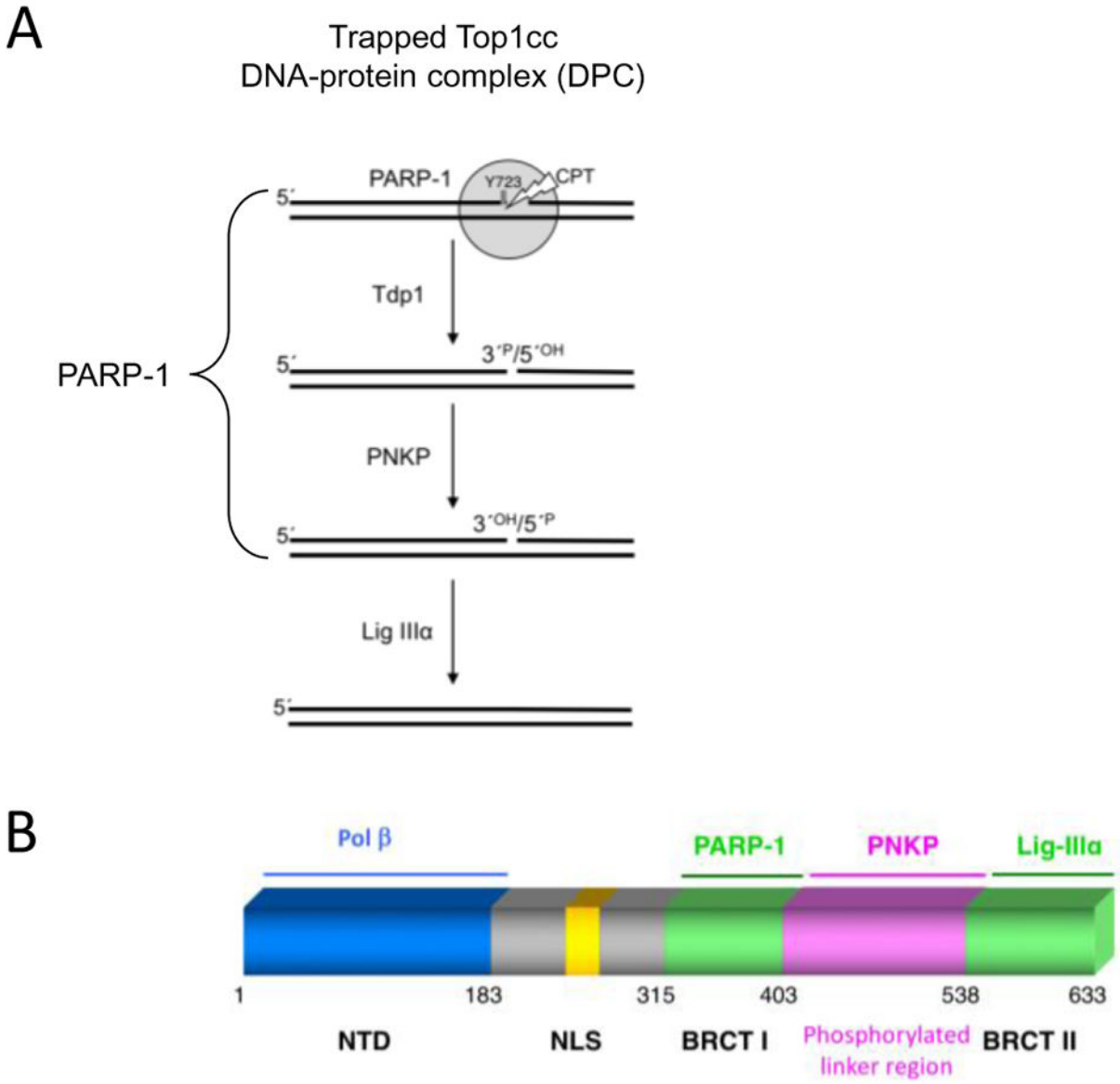

Fig. 1.

(A) Schematic representation of repair of a CPT-trapped Top1cc. (B) Domain organization of mouse XRCC1 indicating the N-terminal domain (NTD) that binds pol β, the BRCT1 domain that interacts with PARP-1, the phosphorylated linker region that binds PNKP and the BRCTII domain that binds and stabilizes lig IIIα.

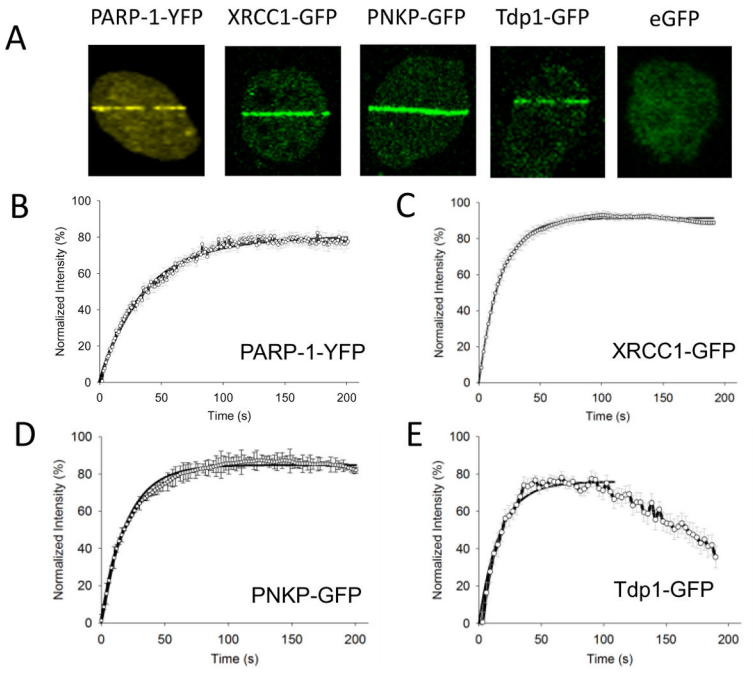

Fig. 2.

Time course of recruitment of transiently expressed C-terminal tagged repair proteins. XC5 cells were subjected to micro-irradiation damage and recruitment was followed for 200 s. (A) Typical accumulation at damaged sites after 100 s for PARP-1-YFP, XRCC1-GFP, PNKP-GFP, Tdp1-GFP and eGFP. Recruitment curves for (B) PARP-1-YFP (n = 20); (C) XRCC1-GFP (n = 30); (D) PNKP-GFP (n = 30) and (E) Tdp1-GFP (n = 15). Transfection and recruitment methods are provided in Materials and Methods. Error bars represent SEM. Fluorescence data were normalized using the intensity at the beginning of recruitment and maximal intensity values, and recruitment kinetics were fitted to 2 exponentials for PARP-1-YFP and single exponentials for XRCC1-GFP, PNKP-GFP and Tdp1-GFP. Half-times for recruitment are compiled in Table 1.

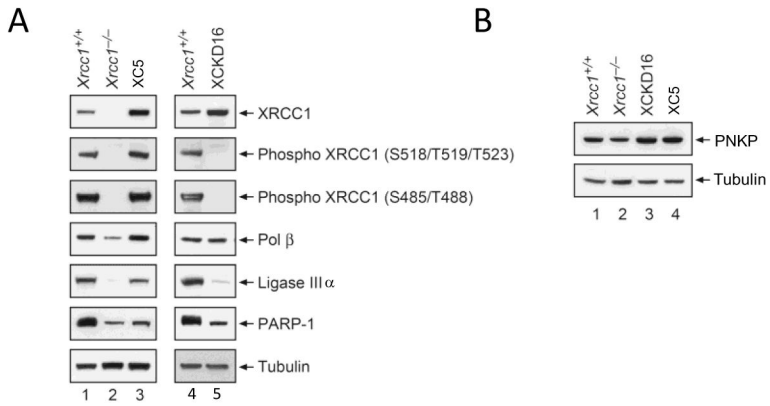

Fig. 3.

Characterization of XCKD16 cells expressing the XRCC1 phosphorylation mutant. (A) Western blotting analysis of XRCC1 and other repair proteins in XCKD16 MEFs compared with *Xrcc1*$^{+/+}$, *Xrcc1*$^{-/-}$ and XC5 cells. (B) Expression of PNKP in the same cell lines. Tubulin was used as a loading control. Full methods are given in Materials and Methods.

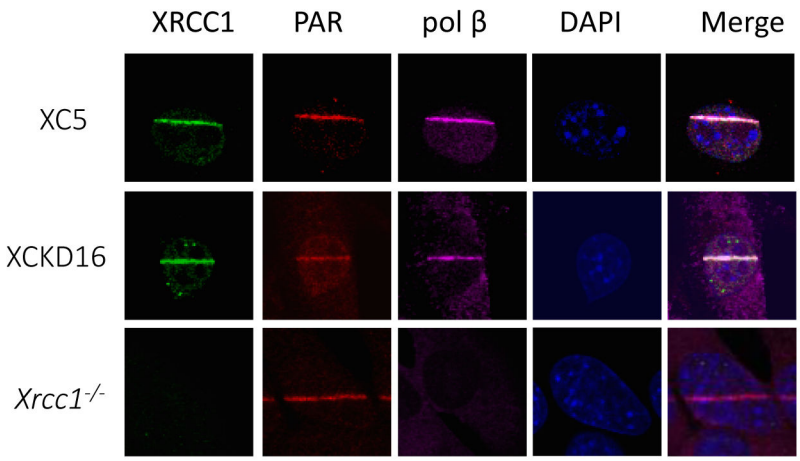

Fig. 4.

Immunofluorescent imaging of XRCC1, PAR and pol β. Cells were micro-irradiated in stripes to initiate XRCC1 and pol β recruitment and synthesis of PAR. After 1 min, cells were fixed and stained and a comparison of representative XC5, XCDK16 and *Xrcc1*$^{-/-}$ cells is shown. Immunofluorescent staining methods are outlined in Materials and Methods.

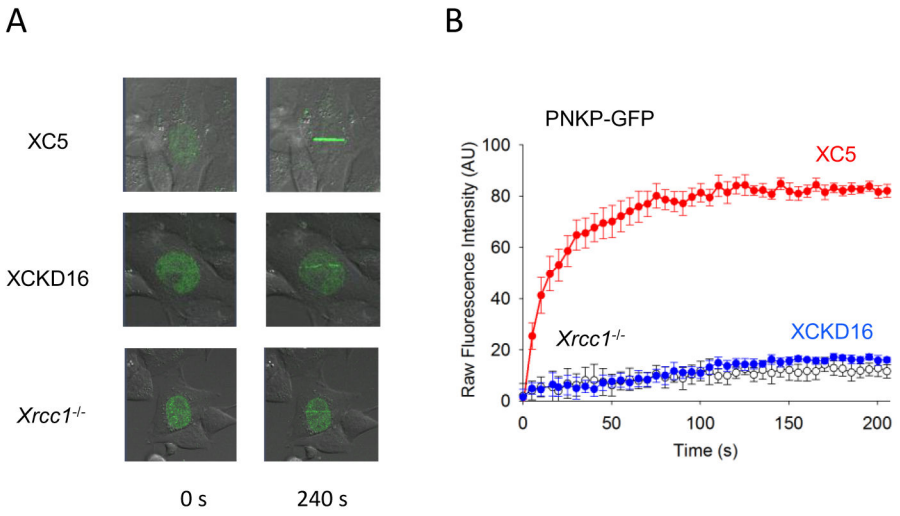

Fig. 5.

Recruitment of transiently expressed PNKP-GFP to micro-irradiation damage sites. (A) Typical accumulation of PNKP-GFP at damaged sites in XC5, XCDK16 and *Xrcc1*$^{-/-}$ cells 0 and 240 s after irradiation. (B) Graphical representation of recruitment. 16–17 cells of each type were analyzed, error bars represent SEM. Experiments and data analysis are described in Materials and Methods.

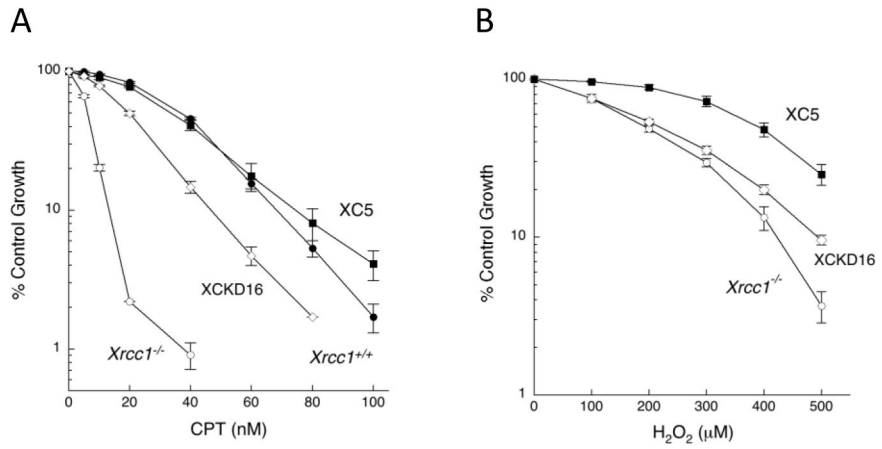

Fig. 6.

Complementation of CPT and H_2O_2 hypersensitivity of *Xrcc1*$^{-/-}$ cells. XC5 or *Xrcc1*$^{+/+}$, XCDK16 and *Xrcc1*$^{-/-}$ cells were compared for sensitivity to (A) CPT exposure and (B) H_2O_2 exposure. Cells were treated with a range of concentrations of CPT for 24 h or H_2O_2 for 1 h, washed and allowed to grow until control, untreated cells reached approximately 80% confluence. Full methods for growth inhibition assays are given in Materials and Methods. Plotted are mean ± SEM values obtained from at least 3 independent experiments.

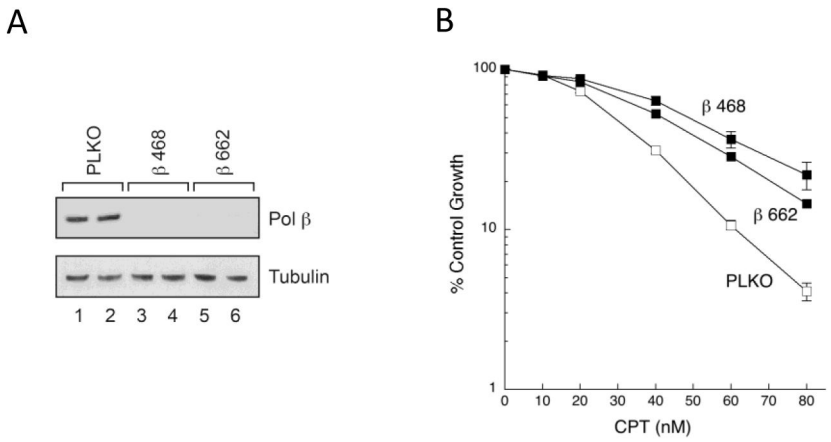

Fig. 7.

Knock down of pol β in XCKD16 cells. XCKD16 cells were transduced with control and β shRNA lentivirus particles. (A) Characterization of pol β expression by western blotting as described in Materials and Methods. Shown are results with control PLKO and two pol β shRNA. Lentivirus was transduced at a MOI of 5 (lanes 1, 3 and 5) or 25 (lanes 2, 4 and 6). (B) Sensitivity of cells (MOI 25) to a 24 h exposure to CPT. Full methods for growth inhibition assays are given in Materials and Methods. Plotted are mean ± SEM values obtained from 3 independent experiments (2 experiments for β 662).

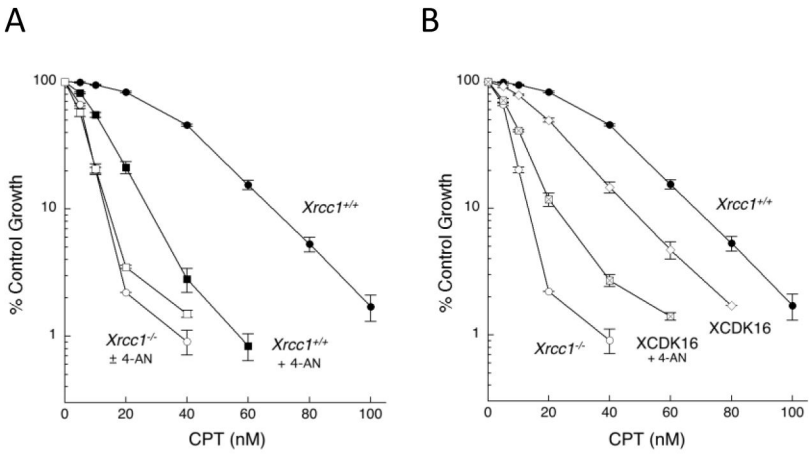

Fig. 8.

Sensitization by PARP inhibition. Cells were treated for 24 h with a range of concentrations of CPT in the absence or presence of the PARPi 4-AN (5 μM). (A) Effect of 4-AN in *Xrcc1*$^{+/+}$ and *Xrcc1*$^{-/-}$ cells, (B) Effect of 4-AN in XCDK16 cells. Growth inhibition assays are described in Materials and Methods. Plotted are mean ± SEM values obtained from at least 3 independent experiments.

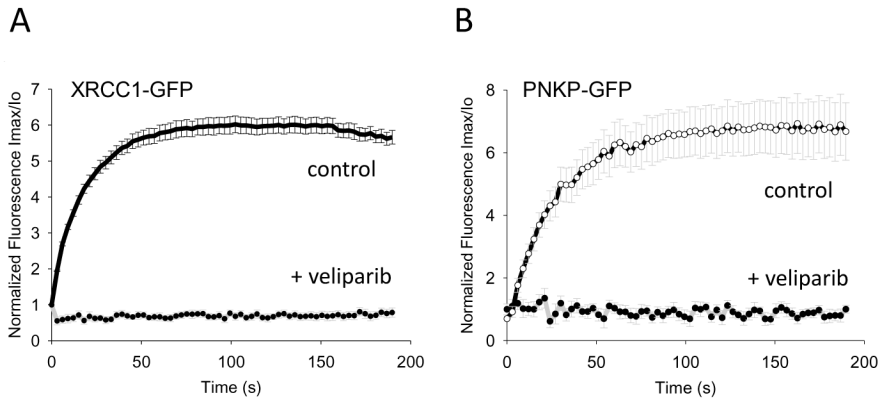

Fig. 9.

Effect of PARP inhibition on recruitment of transiently expressed GFP-tagged proteins. Transfected XC5 cells were pre-treated for 1 h with PARPi, then irradiated in stripes. Recruitment of (A) XRCC1-GFP and (B) PNKP-GFP was followed for 200 s in the absence or presence of veliparib (10 μM). At least 16 cells of each transfection and treatment condition were analyzed, error bars represent SEM. Experiments and data analysis are described in Materials and Methods.

Table 1

Recruitment half-times for tagged repair proteins in XC5

Repair Protein	Recruitment Half-time (s)	Curve Fit[#]
PARP-1-YFP (n=20)	(fast) 4.3 ± 1.0	double exponential 13% of amplitude
PARP-1-YFP (n=20)	(slow) 26.8 ± 0.6	double exponential 77% of amplitude
XRCC1-GFF (n=30)	11.1 ± 0.1	single exponential
PNKP-GFP (n=30)	13.6 ± 0.2	single exponential
Tdp1-GFP (n=15)	11.6 ± 0.7	single exponential
Pol β-GFP (n=30)	11.1 ± 0.2	single exponential [*]

Recruitment curves shown in

[#] Figure 2 and

[*] Figure S3.

Table 2

Increased CPT resistance in XRCC1-expressing cells

Cell line	Fold resistance
XRCC1 WT	5.8
Xrcc1$^{+/+}$	5.6
XCKD16	3.6
Xrcc1$^{-/-}$	1.0

Table 3

Sensitization by 4-AN*

Cell line	MMS#	CPT
Xrcc1$^{+/+}$	2.2	2.5
XCKD16	nd	2.1
Xrcc1$^{-/-}$	15	0

* Fold sensitization (5 μM for 24 h)

Ref [55]